Supplementary information

Enhancing the Electrical Properties and Surface Uniformity of a Copper-Coated Carbon Nanotube Fiber by Optimizing Copper Electrodeposition

Eunsoo Shim, Serin Park, Chaeyun Kim, and Jae-Hong Lim*

Department of Materials Science and Engineering, Gachon University, Seongnam-si, Gyeonggi-do 13120, Republic of Korea.
E-mail: limjh@gachon.ac.kr

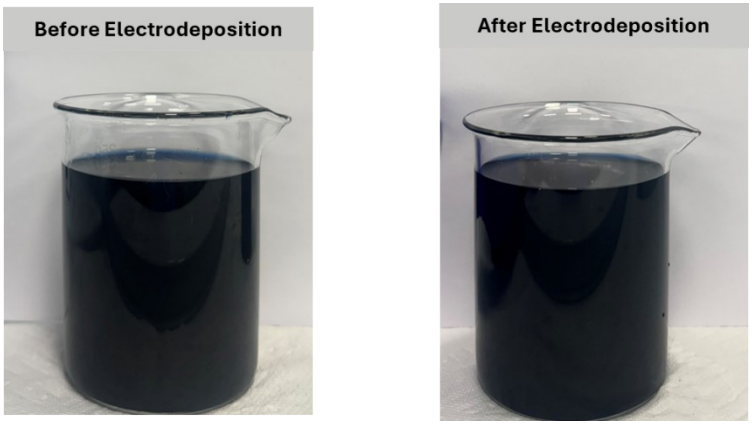

Fig. S1 Photographs of the Cu electrodeposition bath containing 600 ppm HCl (hundreds-of-ppm chloride level) showing a clear solution with no visible turbidity or crystalline CuCl precipitation before and after electrodeposition under the operating conditions used in this study.

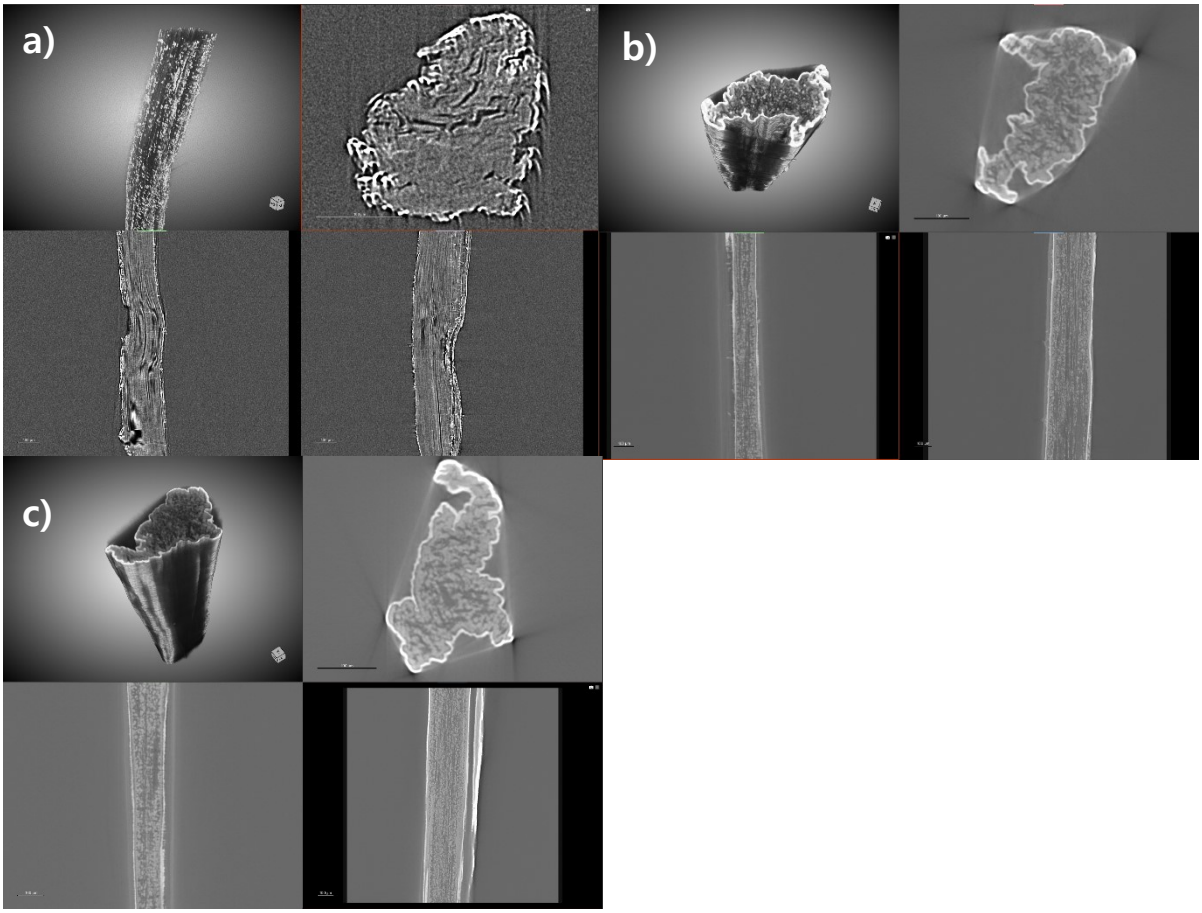

Fig. S2 XRM images of (a) the bare CNT fiber, (b) the Cu-CNT fiber plated with 2 ppm JGB, and (c) the Cu-CNT fiber plated with 10 ppm JGB.

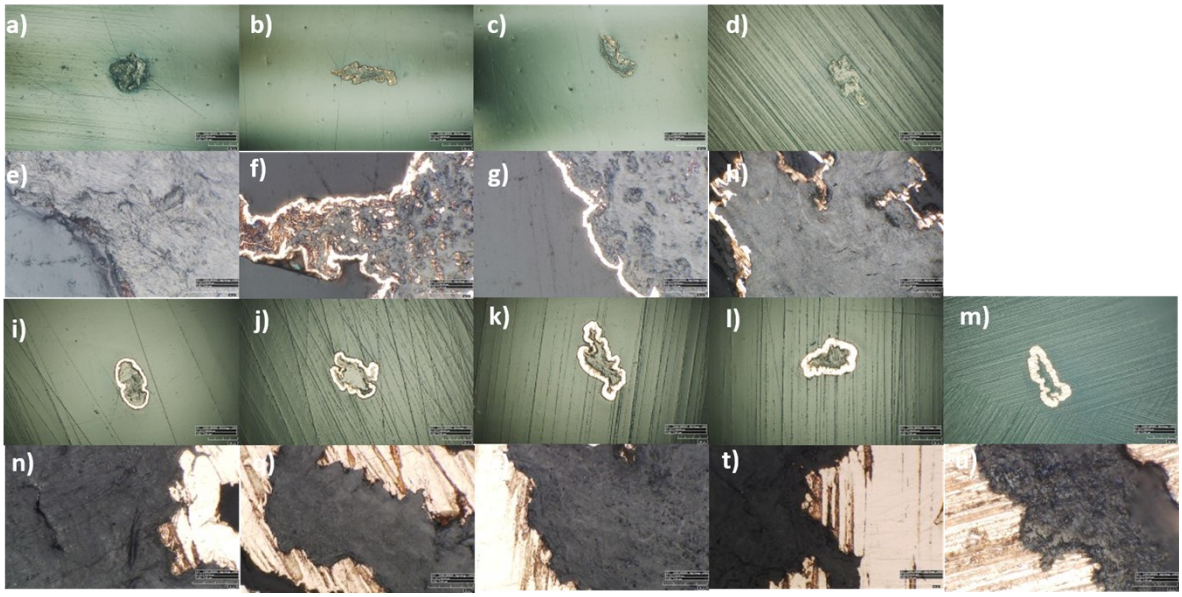

Fig. S3 Plating morphology at various applied potentials (from −0.01 to −0.25 V (vs. Ag/AgCl)) and a JGB concentration of 2 ppm. Lower voltages promoted internal filling, whereas higher voltages produced thicker copper layers on the surface. Optical (200×) and cross-sectional (3000×) images are shown for samples electrodeposited at (a, e) −0.01 V, (b, f) −0.03 V, (c, g) −0.05 V, (d, h) −0.10 V, (i, n) −0.16 V, (j, q) −0.20 V, (k, s) −0.22 V, (l, t) −0.24 V, and (m, u) −0.25 V.

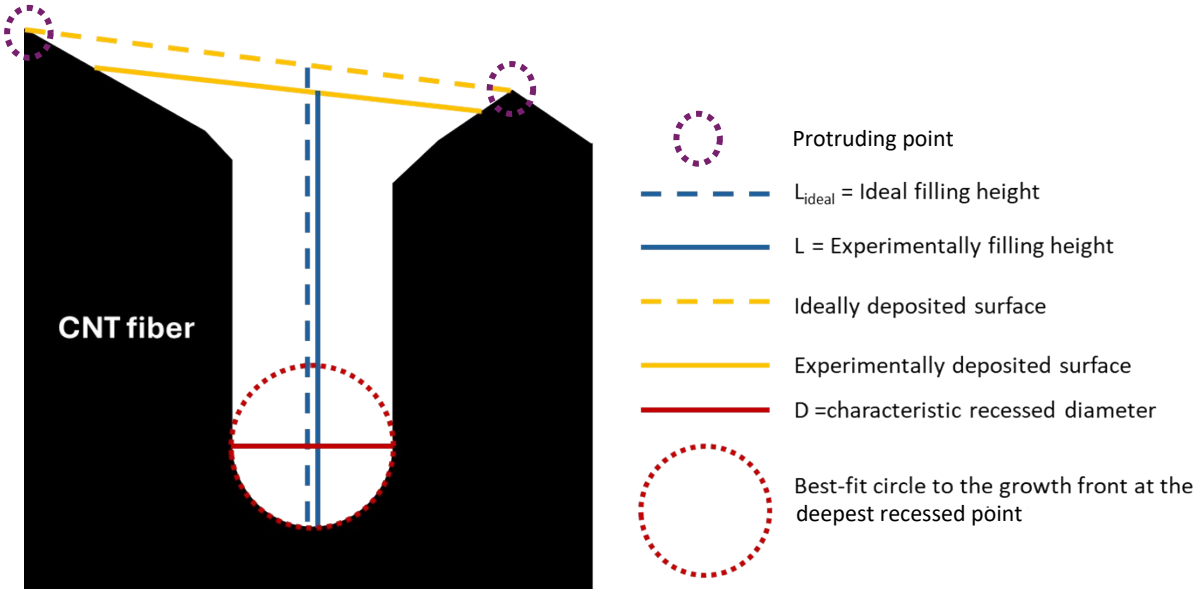

Fig. S4 Schematic defining the geometric parameters used to quantify surface leveling and deposition range and Fig. 7. The characteristic recessed diameter D is obtained as the diameter of the best-fit circle to the growth front at the deepest recessed point. The experimentally measured filling height L is the distance from the deepest recessed point to the experimentally deposited surface, and the ideal filling height L_{ideal} defined relative to the ideally deposited surface. The deposition range is defined as $DR = L/D$.

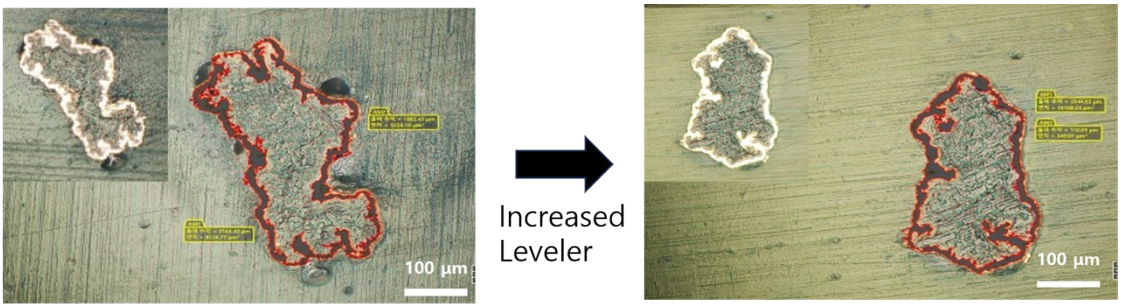

$$w - \underbrace{(A \times l \times \rho)}_{Ext.} = \text{Int.}$$

w: weight of deposited Cu
A: surface area of external Cu layer
l: length of deposited CNT-fiber
ρ: density of Cu ($8.94\ g/cm^3$)
$Int.$: weight of deposited Cu inside $CNT - fiber$
$Ext.$: weight of deposited Cu outside $CNT - fiber$

	External Cu (at%)	Internal Cu (at%)
Low leveler content	76	24
High Leveler content	**62**	**38**

Fig. S5 Cross-sectional images of the samples used for internal filling analysis, along with the calculated internal and external filling ratios as a function of additive concentration. The internal filling ratio also increased as the additive content increased, indicating improved internal deposition.

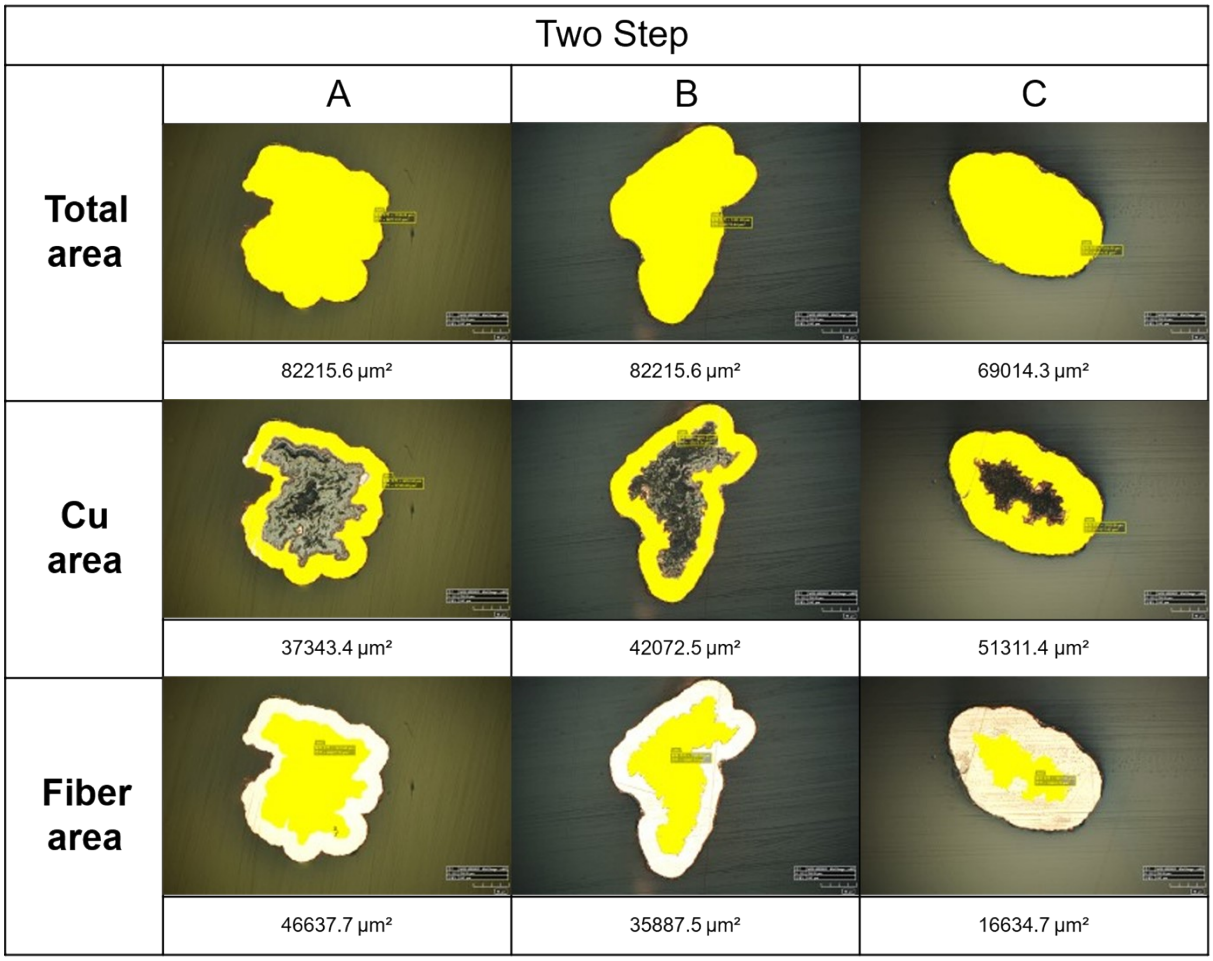

Fig. S6 Optical microscopy image of the cross-section of the specimen used for electrical conductivity measurements; the cross-sectional area determined from this image was used to calculate the electrical conductivity.

Table S1. Electrical conductivity analysis for individual Cu-CNT fiber specimens (A–C) based on four-point probe measurements. The conductivity of three representative specimens is 2.35 ± 0.26 × 10^7 S /m (n = 3), corresponding to a relative standard deviation of approximately 11%.

Sample	Tex (g/km)	Density (g/cm^3)	Total Area (m^2)	Resistance (Ω)	Resistivity (Ω m)	Electrical conductivity (S/m)	Specific Electrical Conductivity (Sm^2/kg)	Limit current (A)	Limit current density (A/cm^2)
A	484.34	5.59	8.67×10^{-8}	0.004928	4.27×10^{-8}	2.34×10^{7}	4189.66		
B	468.75	5.70	8.22×10^{-8}	0.005785	4.76×10^{-8}	2.10×10^{7}	3687.61		
C	464.36	6.73	6.90×10^{-8}	0.005558	3.84×10^{-8}	2.61×10^{7}	3874.59	7.3495	1.07×10^{4}

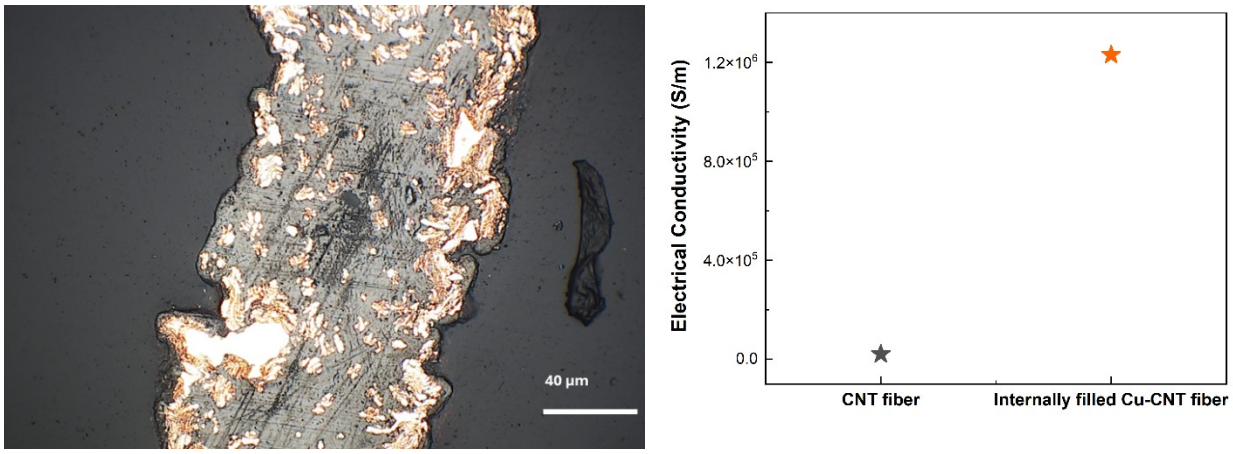

Fig. S7 An internally filled Cu-CNT fiber without an outer Cu layer exhibits an electrical conductivity of 1.23×10^6 S/m, higher than that of bare-CNT fibers electrical conductivity (2.01×10^4 S/m).

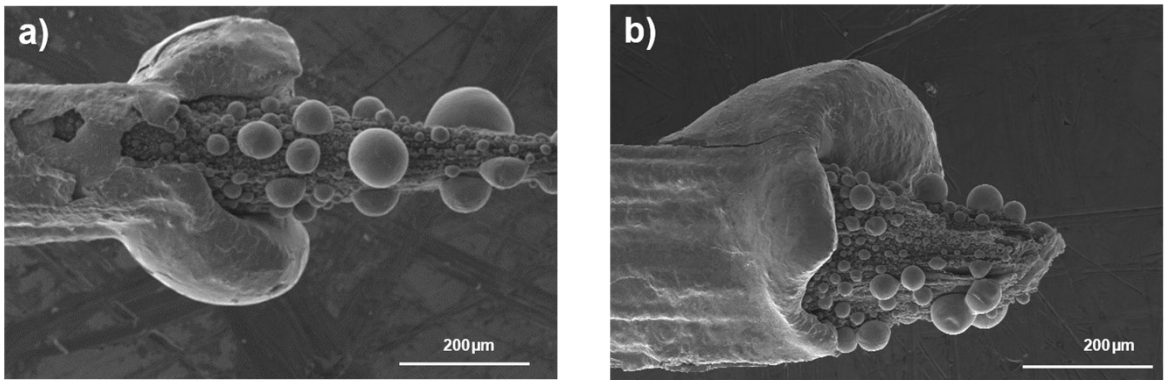

Fig. S8 SEM image of the cross-section of a sample after failure following the current limiting test. Examination of the fractured region revealed Cu particles within the CNT fiber pores, confirming internal filling. This suggests that eliminating internal voids prevented air pocket rupture from heat generation, thereby increasing the current limitation.

.

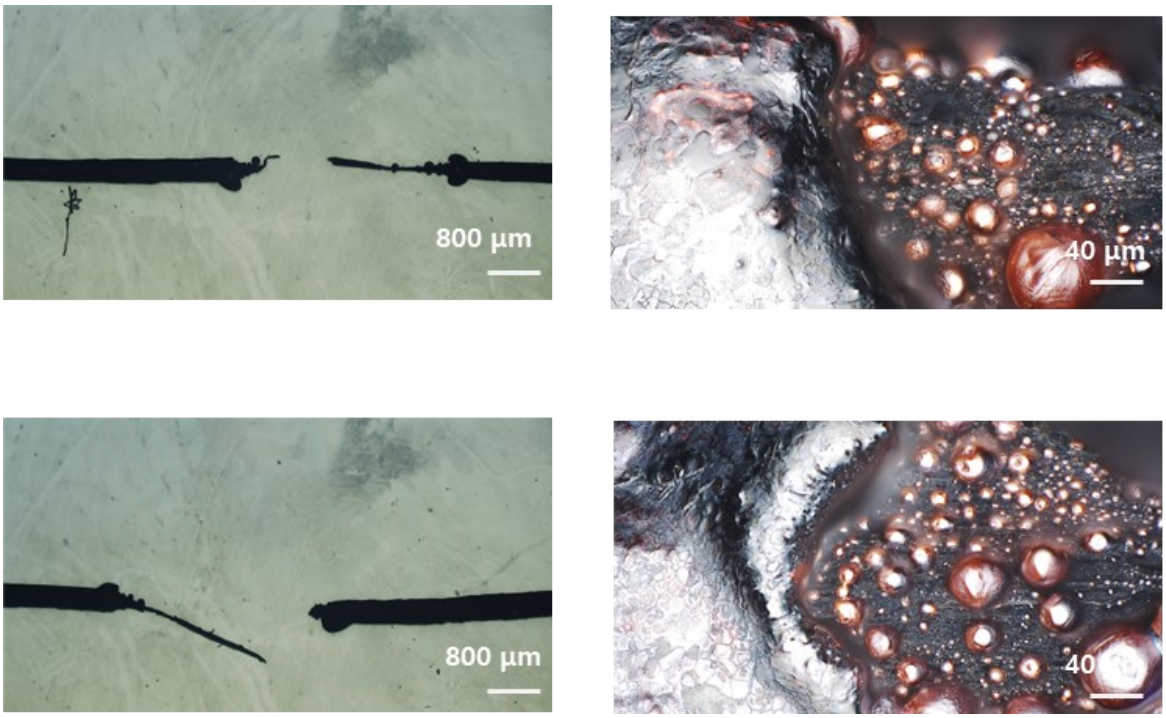

Fig. S9 Optical microscopy images of the fractured surface of the sample after the limiting current test. Copper-colored particles within the CNT fiber provide direct evidence of internal copper filling and confirm effective pore elimination.

Table S2. Summary of uniaxial tensile properties for bare CNT fibers and Cu-CNT fibers prepared by two-step Cu electrodeposition in electrolyte Bath E (JGB = 10 ppm) (*n* = 3 per group) and Cu wires measured in this work for reference (*n* = 3). Engineering tensile strength was calculated using the measured initial cross-sectional area of each specimen. Young's modulus was obtained by linear regression of the initial quasi-linear region after excluding the toe response (ε = 0.001–0.005 for CNT and Cu-CNT fibers; ε = 0.0001–0.0005 for Cu wire). Elongation at break is reported as engineering strain (gauge length = 30 mm), and displacement at break is the corresponding extension at fracture.

No.	Material Name	Cross Section area	Tensile Strength	Young's modulus	Elongation	Displacement at break
		㎟	MPa	GPa	%	mm
1	Bare CNT fiber 1	0.023	75.33	4.69	5.20	1.560
2	Bare CNT fiber 2	0.028	71.53	8.02	9.01	2.703
3	Bare CNT fiber 3	0.025	73.77	10.71	9.01	2.703
1	Cu-CNT fiber 1	0.028	162.01	32.67	8.37	2.510
2	Cu-CNT fiber 2	0.034	126.45	18.51	4.40	1.321
3	Cu-CNT fiber 3	0.034	135.49	22.90	1.09	0.328
1	Cu wire 1	0.053	126.04	114.44	29.54	8.862
2	Cu wire 2	0.053	125.74	147.74	29.54	8.861
3	Cu wire 3	0.053	126.03	124.34	30.62	9.187

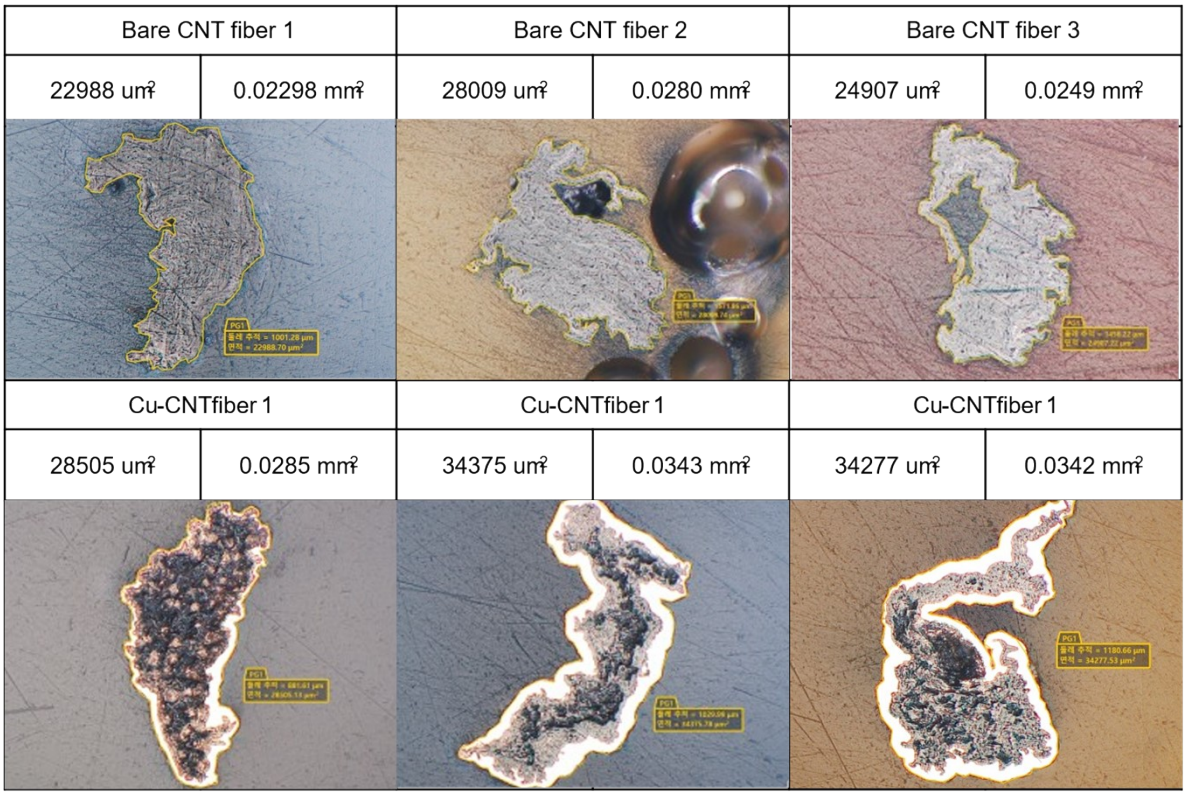

Fig. S10 Optical microscopy cross-sectional images of the fibers used for uniaxial tensile testing. (a–c) Bare CNT fibers and (d–f) Cu-CNT fibers prepared by two-step Cu electrodeposition in electrolyte Bath E (JGB = 10 ppm). The outlined regions indicate the measured *apparent* cross-sectional areas used to calculate engineering stress (Table S2).

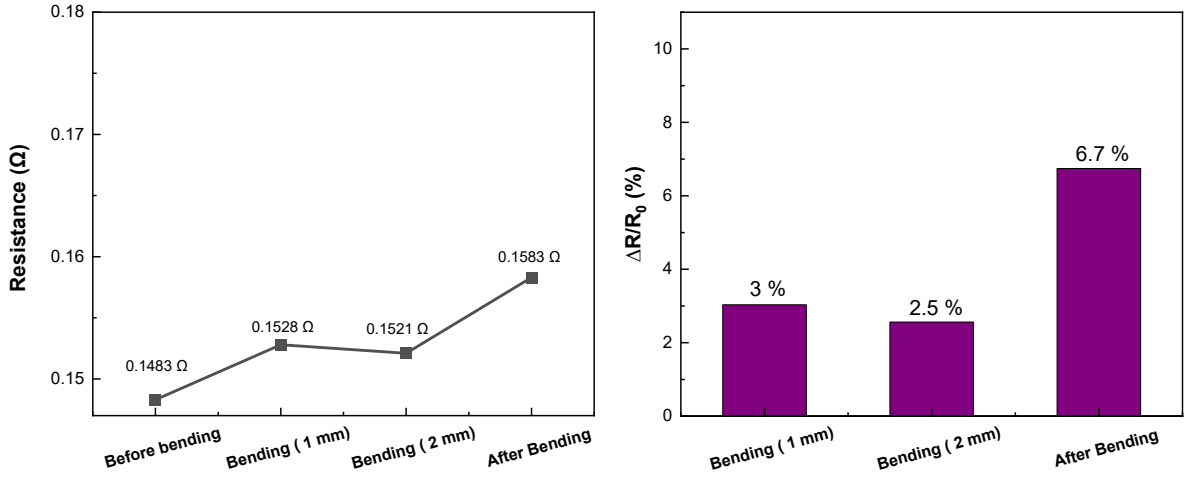

Resistance (Ω)			
Before	Bending (1 mm)	Bending (2 mm)	After
0.1483	0.1528	0.1521	0.1583

Resistance change, ΔR			
Resistance variation (Ω)	0.0045	0.0038	0.0100
Percentage change (%)	3.0344	2.5624	6.7431

Fig. S11 Resistance stability of the Cu-coated CNT fiber under bending and handling. The left panel shows the absolute resistance measured before bending, after bending around rods with diameters of 1 and 2 mm, and after bending/handling. The right panel shows the normalized resistance change, $\Delta R/R_o$ (%), where R_o is the initial resistance before bending. The tables summarizes the corresponding resistance values, ΔR, and percentage changes, with a maximum increase of 6.7% relative to R_o after bending/handling.